Science of Remote Sensing 4 (2021) 100035

Contents lists available at ScienceDirect

Science of Remote Sensing

journal homepage: www.sciencedirect.com/journal/science-of-remote-sensing

Changes in the grasslands of the Caucasus based on Cumulative Endmember Fractions from the full 1987–2019 Landsat record

Katarzyna Ewa Lewińska [a,*], Johanna Buchner [a], Benjamin Bleyhl [b], Patrick Hostert [b,c], He Yin [a,d], Tobias Kuemmerle [b,c], Volker C. Radeloff [a]

[a] SILVIS Lab, Department of Forest and Wildlife Ecology, University of Wisconsin-Madison, 1630 Linden Drive, Madison, WI 53706, USA
[b] Geography Department, Humboldt-Universität zu Berlin, Unter den Linden 6, 10099, Berlin, Germany
[c] Integrative Research Institute on Transformations of Human-Environment Systems (IRI THESys), Humboldt-Universität zu Berlin, Unter den Linden 6, 10099, Berlin, Germany
[d] Department of Geography, Kent State University, 325 S. Lincoln Street, Kent, OH 44242, USA

ARTICLE INFO

Keywords:
Time series analysis
Rangelands
Spectral mixture analysis (SMA)
LandTrendr
Degradation
Google earth engine

ABSTRACT

Grasslands are important for global biodiversity, food security, and climate change analyses, which makes mapping and monitoring of vegetation changes in grasslands necessary to better understand, sustainably manage, and protect these ecosystems. However, grassland vegetation monitoring at spatial and temporal resolution relevant to land management (e.g., ca. 30-m, and at least annually over long time periods) is challenging due to complex spatio-temporal pattern of changes and often limited data availability. Here we assess both short- and long-term changes in grassland vegetation cover from 1987 to 2019 across the Caucasus ecoregion at 30-m resolution based on Cumulative Endmember Fractions (i.e., annual sums of monthly ground cover fractions) derived from the full Landsat record, and temporal segmentation with LandTrendr. Our approach combines the benefits of physically-based analyses, missing data prediction, annual aggregations, and adaptive identification of changes in the time-series. We analyzed changes in vegetation fraction cover to infer the location, timing, and magnitude of vegetation change episodes of any length, quantified shifts among all ground cover fractions (i.e., green vegetation, non-photosynthetic vegetation, soil, and shade), and identified change pathways (i.e., green vegetation loss, desiccation, dry vegetation loss, revegetation green fraction, greening, or revegetation dry fraction). We found widespread long-term positive changes in grassland vegetation (32.7% of grasslands), especially in the early 2000s, but negative changes pathways were most common before the year 2000. We found little association between changes in green vegetation and meteorological conditions, and varied relationships with livestock populations. However, we also found strong spatial heterogeneity in vegetation dynamics among neighboring fields and pastures, demonstrating capability of our approach for grassland management at local levels. Our results provide a detailed assessment of grassland vegetation change in the Caucasus Ecoregion, and present an approach to map changes in grasslands even where availability of Landsat data is limited.

1. Introduction

Grassland ecosystems cover more than a quarter of the global land area (FAO, 2005), and directly support the wellbeing of more than one billion people (Neely et al., 2009). Most grasslands are located in arid, semi-arid, and sub-humid regions (UNCCD, 1994) and are subjected to a combination of diverse global, regional, and local scale processes, such as climate change (Stanimirova et al., 2019) and changes in land use which together results in a complex spatio-temporal pattern of grassland vegetation dynamics. At the global scale, many grasslands are subjected to degradation (Cherlet et al., 2018; IPBES, 2018; O'Mara, 2012), which leads to the loss of biodiversity, threats to food security, and economic susceptibility (IPCC, 2019; UNCCD, 2017a), but at the same time in other regions grassland vegetation is recovering, or 'greening' (e.g., de Jong et al., 2012; Miao et al., 2021; Munier et al., 2018). Mapping and understanding the dynamics of all vegetation changes in grasslands is instrumental to track Land Degradation Neutrality, curb climate change (Cowie et al., 2018; IPBES, 2018; UNCCD, 2017b) and achieve the

* Corresponding author.
E-mail address: lewinska@wisc.edu (K.E. Lewińska).

https://doi.org/10.1016/j.srs.2021.100035
Received 16 June 2021; Received in revised form 2 November 2021; Accepted 9 November 2021
Available online 11 November 2021
2666-0172/© 2021 The Authors. Published by Elsevier B.V. This is an open access article under the CC BY-NC-ND license (http://creativecommons.org/licenses/by-nc-nd/4.0/).

Sustainable Development Goals.

Maintaining grasslands as a natural resource requires monitoring aboveground green vegetation biomass and grassland composition combined with land use history. Grassland vegetation dynamics reflects the interplay between typically broad-scale natural processes and mostly small- and medium-scale anthropogenic changes (Cherlet et al., 2018; IPBES, 2018; IPCC, 2019). Each process has its own timing and length and can result in positive, as well as negative changes in grassland vegetation productivity and composition. However, analyses of grassland vegetation dynamics are often limited to detection of long-term trends (≥10 years) (definition adopted after de Jong et al., 2012) at moderate to low spatial resolution, and lack the routine of high- to medium-resolution monitoring of short-term changes that is typical for, for example, forests (Reinermann et al., 2020). This is unfortunate, because grasslands are heterogeneous and short-term (<10 years) and small-scale changes are important aspects of grassland dynamics, and important for land management in need of informed and timely actions. For example, in regions with increasing human pressure, more frequent short-term droughts (De Keersmaecker et al., 2015) and temperature anomalies can cause small-scale short-term vegetation loss that may ultimately result in widespread and long-term degradation when not mitigated in time. Moreover, grassland monitoring that captures small-scale and short-term changes could support restoration efforts by highlighting vegetation recovery due to shifts in ecosystem functioning (Horion et al., 2016; Zhu et al., 2016) or changes in management and land use intensity (Dara et al., 2020) including optimized grazing (Miao et al., 2021). Consequently, monitoring short- and long-term grassland vegetation dynamics at medium resolution is important to optimize ecosystem services and to track greenhouse gas emissions and global carbon balance (IPBES, 2018; IPCC, 2019).

Remote sensing is an effective approach to monitor grassland ecosystems at different spatial extents (from local to global) and temporal scales (e.g., Ali et al., 2016; Zhou et al., 2017). Vegetation changes in grasslands are frequently approximated through proxy measures of green vegetation biomass (e.g., Zhang et al., 2018; Zhou et al., 2017) calculated based on vegetation indices, such as the NDVI (e.g., Miao et al., 2021) or LAI (e.g., Munier et al., 2018). However, physically-based approaches, such as Spectral Mixture Analyses, are more suitable for monitoring grassland ecosystems, because they provide more reliable results for sparse vegetation (Elmore et al., 2000; Hostert et al., 2003). Moreover, Spectral Mixture Analyses offer concurring insight into grassland ground cover composition and green vegetation productivity (a surrogate of net primary productivity), which broadens capacity of land monitoring (Masiliunas et al., 2021). Spectral unmixing of dense time series of satellite data (e.g., MODIS) allows the calculation of Cumulative Endmember Fractions, that is the annual sums of monthly ground cover fractions (Lewińska et al., 2020). This approach combines benefits of physically-based measurements, quantification of grassland ground cover and the calculation of robust annual estimates by summing the observation for each year (Hobi et al., 2017; Reed et al., 1994).

Grassland ecosystems monitoring with remote sensing often faces tradeoffs between the length of the data time series, frequency of image acquisition, spatial coverage and spatial resolution. Regional to global studies typically apply trend analyses based on long time series of vegetation indices at coarse spatial resolution (Munier et al., 2018; G. Zhang et al., 2018; R. Zhang et al., 2018), or compare modelled and observed grassland productivity at coarse resolution (Zhang et al., 2021; Zhou et al., 2017). Spatially detailed studies typically analyze proxies for small areas (Tepanosyan et al., 2017; Wiesmair et al., 2016), or up to few years (Griffiths et al., 2020) (but see Dara et al. (2020)). Analyses of coarse-resolution satellite allow to identify 'hotspots' of long-term changes, but do not capture fine-scale processes and their drivers, which limits the value of broad-scale assessments for identifying sustainable land management strategies (Reed et al., 2011). Conversely, detailed analyses for small areas, are difficult to conduct for large areas. Medium-resolution satellite data (10–30-m) are thus the most suited to evaluate land management practices in grasslands (e.g., Griffiths et al., 2020), to compare mapped vegetation changes with ground-truth and socio-economic data (Buenemann et al., 2011), and to evaluate grazing intensity or stocking capacity for each field or pasture (Ali et al., 2016; Reinermann et al., 2020).

The opening of the Landsat archive (Woodcock et al., 2008) combined with computing advancements spurred the development of many novel algorithms taking advantage of long and dense time series of medium resolution satellite data (e.g., Kennedy et al., 2010; Verbesselt et al., 2010; Zhu and Woodcock, 2014). Many of the new approaches can identify short- and long-term changes in time series, allowing on in-depth analyses of vegetation dynamics. However, Landsat time series often suffer from data gaps due to missing acquisitions, sensor defect, cloud cover, cloud shadows, and snow. To overcome these data gaps, Landsat data can be fused with data from other sensors (STARFM; Gao et al., 2015; 2006), aggregated to annual maximum composites (LandTrendr; Kennedy et al., 2010), or seasonal composites (Tindall et al., 2012; Xie et al., 2019), or fitted to harmonic models (FF; Yan and Roy, 2020) (CCDC; Zhu and Woodcock, 2014) (COLD; Zhu et al., 2019). Data compositing and harmonic curve fitting techniques can, however, introduce bias into vegetation change analyses, which are, due to seasonality, often very sensitive to the exact timing of data acquisition (Sonnenschein et al., 2011). Subtle intra- and inter-annual changes can be easily missed by both compositing and harmonic curve fitting techniques, which is especially concerning in grassland ecosystems, and in regions with dynamic land use systems (Lewińska et al., 2020). Time series reconstruction based on local moving windows (e.g., Chen et al., 2004; Eilers, 2003; Schwieder et al., 2016) offer an alternative to compositing or harmonic curve fitting, and fill in data gaps while preserving local variability in the time series.

Our main goal was to develop an approach to monitor short-term (<10 years) and long-term (≥10 years) vegetation changes in grassland ground cover composition and green vegetation productivity from 30-m resolution Landsat data. We built upon our previous development of MODIS-based Cumulative Endmember Fractions and advanced this approach further to allow for analyzing finer spatial-scale process regimes based on the entire Landsat time series while accounting for data gaps. Since Cumulative Endmember Fractions require dense (at least monthly) time series, we predicted missing Landsat data with a weighted Whittaker filter (Eilers, 2003; Kong et al., 2019; Whittaker, 1922). Subsequently, following workflow in Lewińska et al. (2020) we conducted temporal segmentation with LandTrendr (Kennedy et al., 2010) to identify location, frequency, and magnitude of changes in green vegetation fraction cover of three years or more. We chose LandTrendr due to its robustness for trajectory-based change detection and common application to annual data, which matched our study goal. For each change we quantified transitions among all ground cover fractions, thus recognizing shifts in grasslands green vegetation productivity and ground cover composition, herein called change pathways. We implemented our approach by combining existing algorithms and methods and applying them across the Caucasus Ecoregion which has a large variety of grassland ecosystems, management types, and rich legacy of socio-economic transformation. Specifically, our objectives were to: i) map changes in grassland vegetation in the Caucasus Ecoregion from 1987 to 2019, including the location, magnitude, timing, and change pathway of all change episodes; ii) analyze changes in grassland ground cover composition and green vegetation productivity at national and regional levels; iii) relate the observed variability in green vegetation fraction to natural and anthropogenic factors (i.e., weather and grazing pressure, respectively); iv) test if our Landsat-based grassland monitoring approach can detect fine-scale spatial patterns of vegetation change, hence support informed land management.

2. Materials and methods

2.1. Study area

The Caucasus Ecoregion covers 580,000 km^2 between the Black Sea and the Caspian Sea and includes two major mountain ranges of the Greater and the Lesser Caucasus Mountains Chains (Fig. 1). The ecoregion is divided between territories of Armenia, Azerbaijan, Georgia, and parts of Iran, the Russian Federation, and Turkey. Elevation ranges from 28 m b.s.l. to 5,642 m a.s.l.. Average annual precipitation has a strong NW-SE gradient and ranges from 4,100 mm to 300 mm per year. The Caucasus is a global hotspot of biodiversity (Marchese, 2015), with many different landscapes (Zazanashvili et al., 2000), and a variety of grassland ecosystems (Belonovskaya et al., 2016; Zazanashvili et al., 2000), making it a great study area to test our methods.

Agriculture is important in the region (Holland, 2016; O'Loughlin et al., 2007), with a long history of pastoralism (Hovsepyan, 2015) and animal husbandry important for both local economy and identity (Neudert and Allahverdiyeva, 2009). However, the collapse of the Soviet Union in 1991, followed by the hardening of political borders (Armenia, Azerbaijan, Georgia, and the Russian Federation), socio-economic transformation, and a series of local conflicts, decreased population density in the mountains (Radvanyi and Muduyev, 2007; Vinogradova and Gracheva, 2018), and disrupted transhumance practices (e.g., Radvanyi and Muduyev, 2007), leading to more stationary grazing (Didebulidze and Plachtd, 2002; Wiesmair et al., 2016), and abandonment of some summer pastures (Vinogradova and Gracheva, 2018). Concurrently, growing economic demand and socio-economic reforms spurred a rise in livestock numbers in Azerbaijan and the northern Caucasus (Neudert, 2015; Neudert and Allahverdiyeva, 2009). In all countries but Russia, access to pastures is regulated through lease (Hartvigsen, 2013), which combined with limited transhumance create many management challenges (Neudert, 2015) and has resulted in overgrazing in some winter (NACRES, 2013) and summer pastures (Leeuw et al., 2019; Wiesmair et al., 2016). Unfavorable changes in local climate (Elizbarashvili et al., 2017; Shatberashvili et al., 2015) also increased the threat of grassland degradation (Shatberashvili et al., 2015; Tepanosyan et al., 2017). Accordingly, the need to regulate grazing practices is strong (Cabinet Ministers of Azerbaijan, 2008). Indeed, our previous analysis based on MODIS time series showed that on average 9% of grasslands in the region experienced negative changes in grassland vegetation each year between 2001 and 2018 (Lewińska et al., 2020), but those analyses were limited by their coarse resolution (500-m), and missed trends during the 1980s and 1990s.

2.2. Satellite data

We analyzed the entire 1984–2019 Landsat Collection 1 Tier 1 surface reflectance data available in Google Earth Engine (Gorelick et al., 2017) as of early December 2019, which was equivalent to 43,800 scenes acquired over the Caucasus Ecoregion (paths 164 to 176, rows 27 to 35) by Thematic Mapper (TM; Landsat 4 and 5), Enhanced Thematic Mapper (ETM+; Landsat 7) and Operational Land Imager (OLI; Landsat 8). All surface reflectance data had been atmospherically corrected using LEDAPS (TM, ETM+ (Masek et al., 2006)) or LaSRC (OLI (Vermote et al., 2016),), and assessed for snow, cloud and shadow contamination (Foga et al., 2017; Zhu and Woodcock, 2012). We removed pixels flagged as saturated, cloud, cloud shadow, or snow (bits 2–3, 4–6, 7–8, 9–10 in the 'pixel_qa' Quality Assessment band). Finally we combined OLI with TM and ETM+ scenes following Roy et al. (2016).

2.3. Ancillary data

To focus on grasslands only, we used the land cover classifications of Buchner et al. (2020), and Bleyhl et al. (2017). First, we selected from the datasets described in Buchner et al. (2020) a pixel as 'grassland' if it was classified as 'rangeland' or 'barren' in at least 4 out of 6 time-steps (1987, 1995, 2000, 2005, 2010 and 2015; the 2015 classification adjusted producer's accuracy is 0.77 ± 0.03 and 0.71 ± 0.15, and adjusted user's accuracy is 0.89 ± 0.03 and 0.59 ± 0.14, for 'rangeland' and 'barren' classes, respectively). We included the 'barren' class into our grassland definition due to very sparse vegetation cover in some parts of the region. Our multi-temporal grassland definition was motivated by the long analysis period and allowed inclusion of regions that have extremely low vegetation cover, or were misclassified in any of the individual time steps. To cover the entire Caucasus Ecoregion, we used the 2015 land cover dataset from Bleyhl et al. (2017), and especially the 'rangeland' and 'sparse vegetation' classes (producer's accuracy: 0.84 and 0.66; user's accuracy: 0.88 and 0.72, respectively), for the areas not mapped by Buchner et al. (2020).

We analyze meteorological conditions using the TerraClimate time series (Abatzoglou et al., 2018; University of East Anglia Climatic

Fig. 1. Grasslands in the Caucasus Ecoregion based on Buchner et al. (2020) and Bleyhl et al. (2017) (see section 2.3.). Numbered locations are discussed in the text.

Research Unit et al., 2017). Based on the monthly 1984–2019 precipitation and evapotranspiration data at ~4 km (1/24th degree) resolution, we calculated SPEI3 (Standardized Precipitation-Evapotranspiration Index calculated at the time scale of three months) (Vicente-Serrano et al., 2010, 2012) using the SPEI R library (https://cran.r-project.org/web/packages/SPEI). SPEI combines precipitation and evapotranspiration, which together affect aboveground productivity in grassland vegetation (Wang et al., 2014), making SPEI well suited for analyses of vegetation dynamics (De Keersmaecker et al., 2015; Vicente-serrano, 2007). The selected SPEI aggregation period of three months corresponds with the maximum time lag in the response of grassland vegetation to meteorological conditions (Horion et al., 2012). Positive SPEI values indicate favorable vegetation growth conditions, whereas negative values mark dry and hot spells. We summed monthly SPEI3 data for each year akin to the Cumulative Endmember Fractions time series (see section 2.4.).

We obtained regional statistics on livestock numbers from national statistical offices, yearbooks and regional departments (see Table SA.1 for references). We used FAOSTAT (FAO, 2020) statistics for livestock information on a national level. Finally, we digitized active shepherds' camps and enclosures in three sites (6 × 9 km each) representing different grassland types and grazing regimes. For this, we visually interpreted the most recent high-resolution images available in Google Earth as of November 2020. We determined the activity status of each camp by looking for maintained buildings, tents, or dung accumulation (Bleyhl et al., 2019; Dara et al., 2020).

2.4. Landsat based Cumulative Endmember Fractions

We analyzed changes in grassland ground cover using the Cumulative Endmember Fractions introduced by Lewińska et al. (2020). Cumulative Endmember Fractions are annual sums of monthly ground cover fractions (e.g., soil, green vegetation, non-photosynthetic vegetation and shade) that characterize grassland green vegetation productivity (a proxy for net primary productivity), ground cover composition, and structure (i.e., shadow accounts, among others, on micro-shadowing at the sub-pixel level). Summing values by year captures the full range of phenology and illumination conditions (Elmore et al., 2000) and facilitates year-to-year comparisons.

To calculate Cumulative Endmember Fractions, we applied Spectral Mixture Analysis (SMA) to each Landsat scene using four endmembers: soil, green vegetation, non-photosynthetic vegetation, and shade (Fig. 2) assuming their linear combination

$$\rho_j = \sum_{i=0}^{n} f_i * \rho_{i,j} + e_j \quad (1)$$

where, ρ_j is the reflectance in Landsat band j, f_i is a fraction of endmember i, $\rho_{i,j}$ is a spectrum of endmember i in band j, and e_j is a residual term for band j. We applied a constrained and non-negative SMA and used spectra identified by Lewińska et al. (2020) (for details see *ibid.*, sections 2.4 and 2.5). Next, we aggregated the resulting fraction time series to monthly composites selecting for each pixel image that had the highest green vegetation value for each month.

Due to infrequent observations in the early years of Landsat (Figure SB1, SB2, and Table SB1), we started our vegetation change analyses in 1987. Moreover, for 2019 only January–November scenes were available when we conducted our analyses. For months without any Landsat composites, we predicted values for each endmember for each pixel using the Whittaker filter (Atkinson et al., 2012; Eilers, 2003; Whittaker, 1922) as implemented by Kong et al. (2019). The Whittaker filter fits a local curve while preserving the upper envelope, is computationally efficient, and can handle missing observations (Eilers, 2003). Furthermore, unlike other time series reconstruction approaches, the Whittaker filter allows us to weight observations according to, for example, their quality. We calculated monthly inter-annual medians as fill-in values, and gave them a weight of 0.5, while weighting all original observations as 1 (after Kong et al. (2019)). All the original values in the time series were preserved in the final monthly time series, and missing months predicted based on the Whittaker filter (for details and sensitivity analysis see Supplement B.1.).

Based on the complete monthly endmember fraction time series, we calculated Cumulative Endmember Fractions as the annual sum for each respective endmember

$$cef_{iY} = \sum_{m=1}^{m} f_{miY} \quad (2)$$

where, cef_{iY} is Cumulative Endmember Fraction for endmember *i* in year

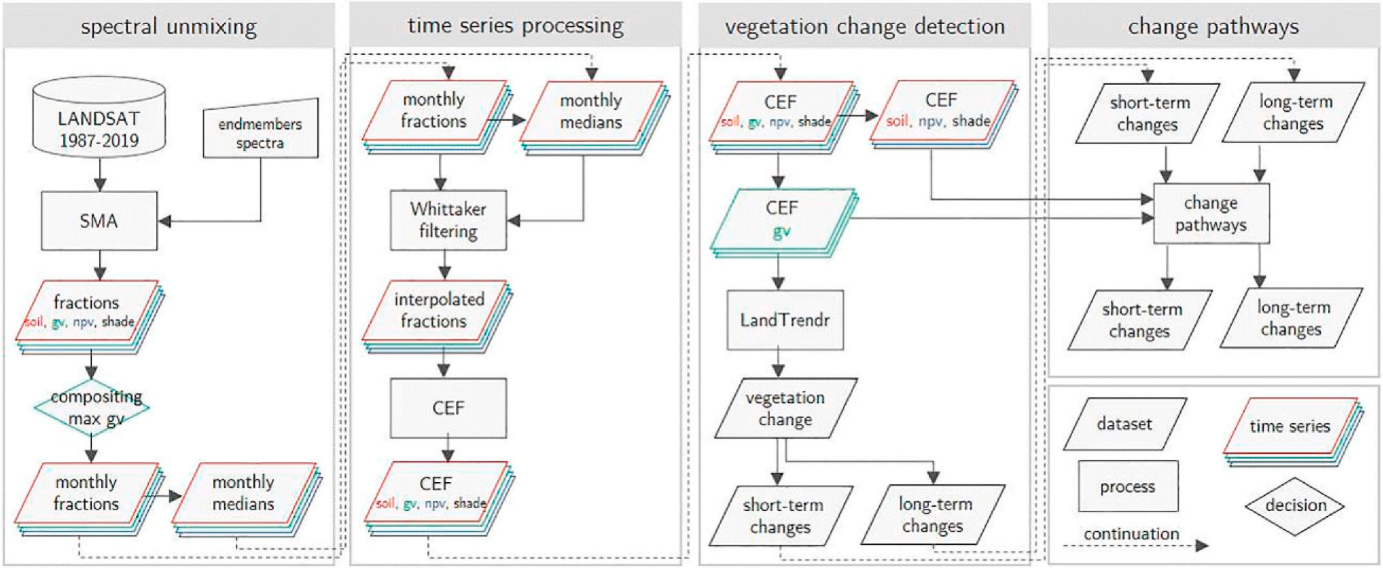

Fig. 2. Data processing workflow including: spectral unmixing of the Landsat time series, aggregation to monthly ground cover fractions, prediction of missing monthly data based on the Whittaker filter, aggregation to the Cumulative Endmember Fractions (CEF), identification of vegetation changes based on LandTrendr, and calculation of change pathways for both short-term and long-term change episodes. The results of each processing block shown in the last row are the input data for the next processing block.

Y, f_{miY} is fraction for endmember i in month m and year Y. To improve interpretability, we rescaled all the Cumulative Endmember Fraction for each year to sum to 100, thus the values represented percentage share of each fraction. Lastly, following Lewińska et al. (2020), we combined non-photosynthetic vegetation and shade Cumulative Endmember Fractions into one cumulative fraction, hereafter 'non-photosynthetic vegetation'.

To identify multi-year change episodes in grasslands vegetation cover, as in Lewińska et al. (2020) we applied the LandTrendr temporal segmentation algorithm to the green vegetation Cumulative Endmember Fraction. We used default control parameters (see Table 1 of Kennedy et al. (2018)), but preserved all spikes, allowed up to 12 segments, and a one-year recovery period. We retained only those vegetation change episodes that were at least three years-long and where the green Cumulative Endmember Fraction increased or decreased by at least 20% of the per-pixel maximum green vegetation Cumulative Endmember Fraction to be conservative, and avoid including minor changes into our trend analyses. To account for co-registration errors and reduce the 'salt and pepper' effect, we applied a minimum mapping unit of 11 pixels (~1 ha).

Finally, we calculated the change pathway for each vegetation change episode i.e., the transitions among green vegetation, non-photosynthetic vegetation, and soil fractions (Fig. 3) between the first and the last year of each episode. The changes approximate percentage point shifts in grassland green vegetation productivity and composition. Specifically, we identified three negative change pathways in vegetation cover (after Lewińska et al. (2020)), i.e., desiccation (a shift from green vegetation to non-photosynthetic vegetation fraction), green vegetation loss (a shift from the green vegetation fraction to soil fraction), and dry vegetation loss (a shift from non-photosynthetic vegetation to soil fraction); and three positive change pathways, i.e., greening (a shift from non-photosynthetic vegetation to green vegetation), revegetating green fraction (a shift from soil to green vegetation), and revegetating dry fraction (a shift from soil to non-photosynthetic vegetation).

2.5. Changes in grassland vegetation cover

We analyzed the location, magnitude, frequency, timing, and change pathways (see above) of all vegetation change episodes, but separated them into long-term (≥10 years) and short-term (3–9 years) changes. We evaluated the accuracy of vegetation change detection by visually assessing 1987–2019 time series of green vegetation Cumulative Endmember Fraction for 850 samples. To do so, we used the AREA^2 tool (available at https://area2.readthedocs.io) to design a stratified random sample aimed at an expected accuracy of 80% (Olofsson et al., 2014; Stehman, 2014). Accordingly, we distributed 250 points within grassland areas that had at least one green vegetation loss episode, and 600 points within grasslands that showed no vegetation change from 1987 to 2019. Without knowing the sampling strata, one skilled interpreter (KEL) divided green vegetation Cumulative Endmember Fraction time series for each sample point into distinct segments with clear temporal trajectories (i.e., increase, decrease or stable).

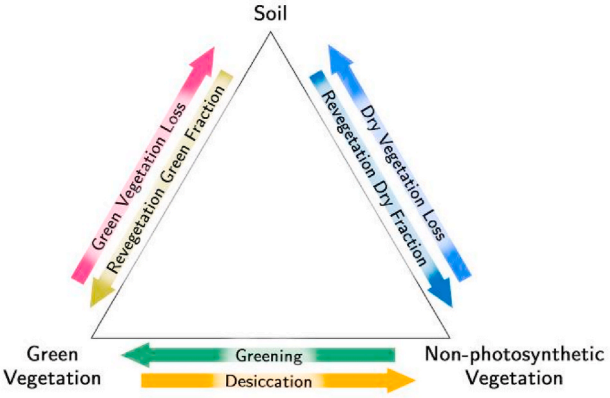

Fig. 3. Change pathways in grassland ground cover composition approximated by soil, green vegetation, and non-photosynthetic vegetation fractions. Figure modified from Lewińska et al. (2020).

For any change segment, we identified years of vegetation change as the period from the segment's start vertex plus one year, through the segments end (short- and long-term, combined, with 1988 being the first year with mapped vegetation change). Next, we compared the original LandTrendr results with the reference dataset and assessed the accuracy of the vegetation change detection separately for each year based on green vegetation loss (yes/no response) accounting for the inclusion probability of the validation sample (Stehman, 2014), and calculated error-adjusted overall, user's, and producer's accuracy, and the adjusted area of change for each year. Finally, we calculated the area of positive and negative changes in vegetation cover at annual basis quantifying contribution of short-term and long-term changes to the overall pattern and reported it separately for all six change pathways on the country level adjusting for accuracy. We decided to focus the evaluation only on vegetation loss because we assumed it would be the dominant process in the region, and implementation of the stratified random sample design accounting for all frequencies of vegetation loss and gain changes across all the years, was not feasible due to the very limited representation of some types of changes.

2.6. Vegetation dynamics versus SPEI3 and livestock populations

We assessed the effects of meteorological conditions on changes in green vegetation Cumulative Endmember Fraction by correlating them with SPEI3. We used 1987–2019 SPEI3 annual sums on pixel level, and rescaled the SPEI3 time series to match the 30-m resolution of Cumulative Endmember Fractions using nearest-neighbor interpolation. Independently, we used parameterized linear regression models to quantify response of green vegetation Cumulative Endmember Fraction to SPEI3 and livestock numbers. We analyzed the statistical relationship for entire countries (Armenia, Azerbaijan and Georgia) and for first-level administrative regions (for Azerbaijan we used economic regions to match the statistical data) to match the available statistical data. Consequently, we calculated average annual SPEI3 and green vegetation Cumulative Endmember Fraction for each administrative region, and related them to livestock statistics. We used both datasets at their original resolution. Specifically, we constructed our models to quantify response of green vegetation Cumulative Endmember Fraction to changes in i) SPEI3 annual sums, ii) annual sheep and goat livestock numbers, and iii) the integration of both SPEI3 and livestock.

2.7. Fine-scale spatial patterns of vegetation change

Finally, to test the potential of our Landsat-based approach for grassland management, we examined 2018 vegetation change spatial patterns for three sites: i) winter camps in Pontic-Caspian steppe in Russia; ii) winter camps in shrub desert steppe on Shirvain plain in Azerbaijan; and iii) summer grazing grounds in The Kaçkar Mountains in Turkey. For each site, we selected five shepherds' enclosures or camps, for which we calculated annual 1988–2019 area of positive and negative vegetation change pathways within 0–250, 250–500, and 500–1,000-m from the camps.

3. Results

3.1. Performance of Whittaker filter for Landsat based Cumulative Endmember Fractions

Our implementation of the Whittaker filter successfully predicted missing monthly values. The filter performance was linearly dependent

on the amount of data in a given year (Figure SB4, Table SB1, Table SB2), and errors were higher when observations from the months of highest endmember fractions were missing. Based on data availability (Figures SB2, Table SB1) the overall prediction error for 1987–2019 Cumulative Endmember Fractions was low to moderate, but errors were somewhat higher in mountains (Figure SB5).

3.2. Short-term and long-term changes in grassland vegetation cover

We found that grassland vegetation across the Caucasus was highly dynamic, with both positive and negative change pathways being widespread, as were both short-term and long-term changes. Negative change pathways (short-term or long-term) affected about 51,800 km^2 of grasslands (20.9% of all grasslands, 8.8% of the ecoregion) and were most widespread in the eastern Caucasus (Fig. 4). About 2,450 km^2 of grasslands (4.7%) underwent more than one negative change episode between 1987 and 2019. Negative change hotspots occurred in the Caspian lowland, around the Mingachevir Reservoir, in Nakhchivan, Gobustan, and the Shirvan plain. Positive pathways affected approximately 81,200 km^2 of grasslands (32.7% of all grasslands, 13.8% of the ecoregion), with 7,700 km^2 (3.2%) having more than one positive change episode. Positive change pathways were most common in the southern and eastern parts of the Caucasus. For about 8.4% of all grasslands (20,900 km^2) we observed at least one sequence of both positive and negative change (in any order). Approximately 55,700 km^2 (22.5%) of grasslands experienced a single positive change episode, without any negative change lasting ≥3 years. Conversely, a single negative change with no positive change episode occurred on 24,500 km^2 (9.9%) of grasslands. Almost 55% of all grasslands (136,700 km^2) in the regions showed no change in vegetation cover between 1987 and 2019. The spatial pattern of changes was heterogeneous with adjacent patches following often very different trajectories.

Among the different vegetation change pathways (Fig. 3), positive change pathways were the most widespread in the region in any given year, and long-term positive changes occurred in around 15% of all grasslands in most years (Fig. 5). Revegetation of green fraction was the dominant long-term positive change pathway, followed by the revegetation of dry fraction. Short-term positive changes were more frequent before 1996 than after, with greening being the most common change pathway since 1996. Short-term revegetation of dry fraction was negligible after 1996. Negative change pathways were more widespread prior to 2000 than after. Long-term negative change pathways were most common in the 1990s when they affected more than 4% of grasslands each year. Desiccation was the dominant negative change pathway, with green vegetation loss coming second. Short-term negative change pathways were most prevalent in 1996–1999 and 2011–2019 with desiccation being the most common.

The overall accuracy of our vegetation change detection ranged from

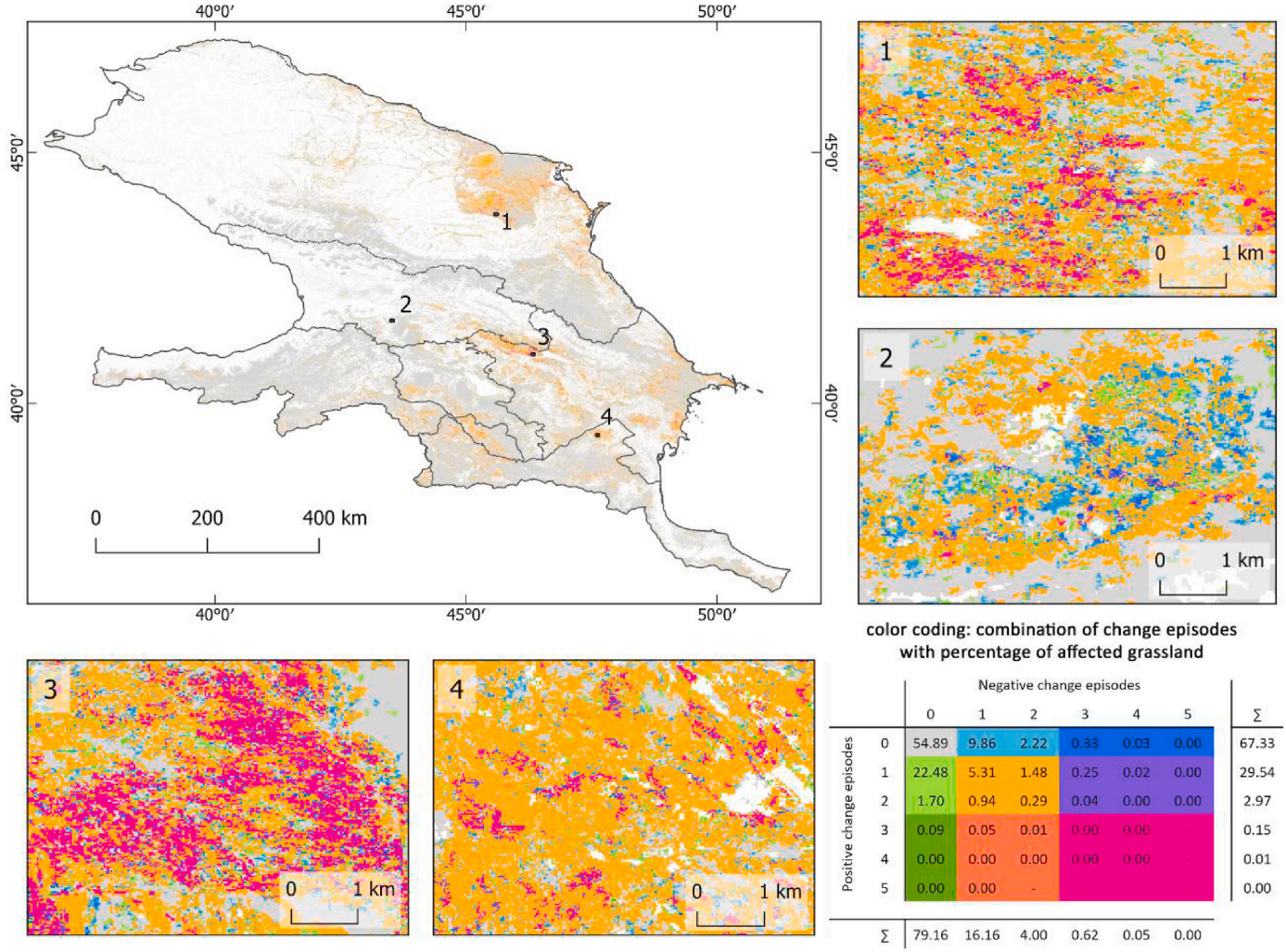

Fig. 4. Number of changes in grassland vegetation composition and green vegetation productivity (short-term and long-term change together) identified between 1987 and 2019. Panels 1–4 show local spatial patterns highlighting the frequency and complexity of changes. The matrix shows a combinations of frequency of positive and negative change episodes, their respective color-coding and the percentage of affected grassland area.

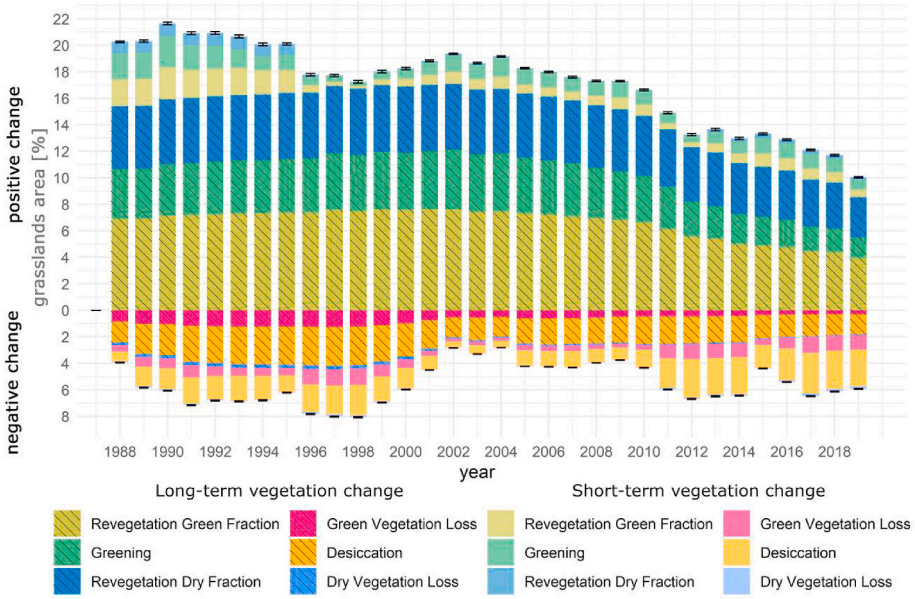

Fig. 5. Annual breakdown of area under short- and long-term vegetation change pathways. Error-adjusted area of vegetation change inTable SA2. Annual vegetation change patterns inFigure SA3. Long- and short-term changes shown separately in Figures SA4and SA5, respectively.

95.8 ± 0.7% to 98.7 ± 0.3% among years (Table SA2). User's accuracy for the vegetation change class was on average 81.7% (ranging between 54.8 ± 6.3% and 93.4 ± 2.3%), and producer's accuracy on average 56% (33.1 ± 7.8% and 78.5 ± 5.8%).

3.3. *Vegetation changes in the different countries*

The area of long-term positive change pathways was generally consistent in all countries through years (Fig. 6). In Azerbaijan and Iran all three positive change pathways were the most abundant between 1997 and 2010. In Russia, the greening pathway increased in area until 2002. Only in Georgia did the area of revegetation green fraction show a steady decline after 1997.

The area affected by long-term negative change pathways decreased over time in the whole Caucasus, with a clear transition point around the year 2002 (Fig. 6). However, not all countries followed the same change trajectory, and disparities occurred among three negative change pathways. In Azerbaijan and Iran, the greatest drop in the area of both long-term green vegetation loss and dry vegetation loss occurred after 2002. Long-term green vegetation loss and dry vegetation loss also decreased in Armenia and Turkey after 2002. In contrast, in Russia and Georgia green vegetation loss and dry vegetation loss were more widespread after 2002. Long-term desiccation decreased over time in most countries, but not in Georgia and Armenia, and was still widespread in Russia and Azerbaijan after 2000. The decrease in area of positive and negative long-term change pathways after 2011 was due to our definition of a long-term change as being at least 10 years in duration, which meant that all new changes detected in the last nine years of the time series were by definition 'short-term'.

Overall, we detected four periods of more widespread short-term negative changes in vegetation cover: 1988–1992, 1996–1998, 2011–2014 and 2017–2018, but there were differences in the extent, magnitude and exact timing among countries. The greatest changes in area of negative changes in grassland vegetation cover occurred in Azerbaijan and Russia, particularly for green vegetation loss and desiccation. Short-term changes in vegetation cover often re-occurred, and the area of positive and negative change pathways frequently fluctuated over time (Fig. 6). Short-term revegetation was, on average, most widespread before 1995 and clearly declined in all countries thereafter. This change was particularly pronounced for green and dry revegetation pathways in Russia, Azerbaijan, and Iran. In Russia the area of short-term greening increased again briefly in the 2000s. Similarly, revegetation of green fraction expanded in the 2000s in Azerbaijan, Russia, and Turkey. Finally, both revegetation pathways became again more abundant after 2012.

3.4. *Effects of SPEI3 and livestock on the green vegetation Cumulative Endmember Fraction*

We found little evidence that the observed changes in grassland vegetation were due to weather. The pixel-based correlations of the green vegetation Cumulative Endmember Fraction versus the SPEI3 1987–2019 time series were mostly insignificant (Figure SA6). However, we observed significant positive correlation in small areas, including the southern part of the Caspian Lowland, west and north of the Mingachevir Reservoir, and in the border region among Turkey, Armenia and Iran. Smaller patches of highly positively correlated pixels occurred on the slopes of Greater and Lesser Caucasus Mountain Chains.

Linear regression models showed in general limited explanatory power of SPEI3 in explaining variability in green vegetation Cumulative Endmember Fraction across the Caucasus (Table SA3-9). In Azerbaijan, Iran, and Turkey, we found no significant relationship between SPEI3 and green vegetation. In Georgia, we found only in the Kvemo Kartli province a significant ($p>0.05$) positive relationship between SPEI3 and green vegetation. In the Russian part of the Caucasus Ecoregion the relation between SPEI3 and green vegetation was moderately strong at best. However, SPEI3 had strong and positive relation to green vegetation in all regions in Armenia.

Effects of small livestock (i.e., sheep and goats) on green vegetation Cumulative Endmember Fraction differed considerably among regions. In Azerbaijan, the relation was slightly positive at the country level and in three of its regions. The same was true in Chechnya in Russia, where we also detected a significant positive relation. Conversely, in Gumushane and Erzincan in Turkey we found a significant negative relationship. In Armenia, Georgia, and in most of the administrative regions in Turkey the relationship between green vegetation and livestock was insignificant. The same was true in Iran, but that may be due to the quality of Iran's livestock data (Figure SA13).

Multivariate models including both SPEI3 and livestock were mostly insignificant ($p>0.05$), or their explanatory power was lower than for

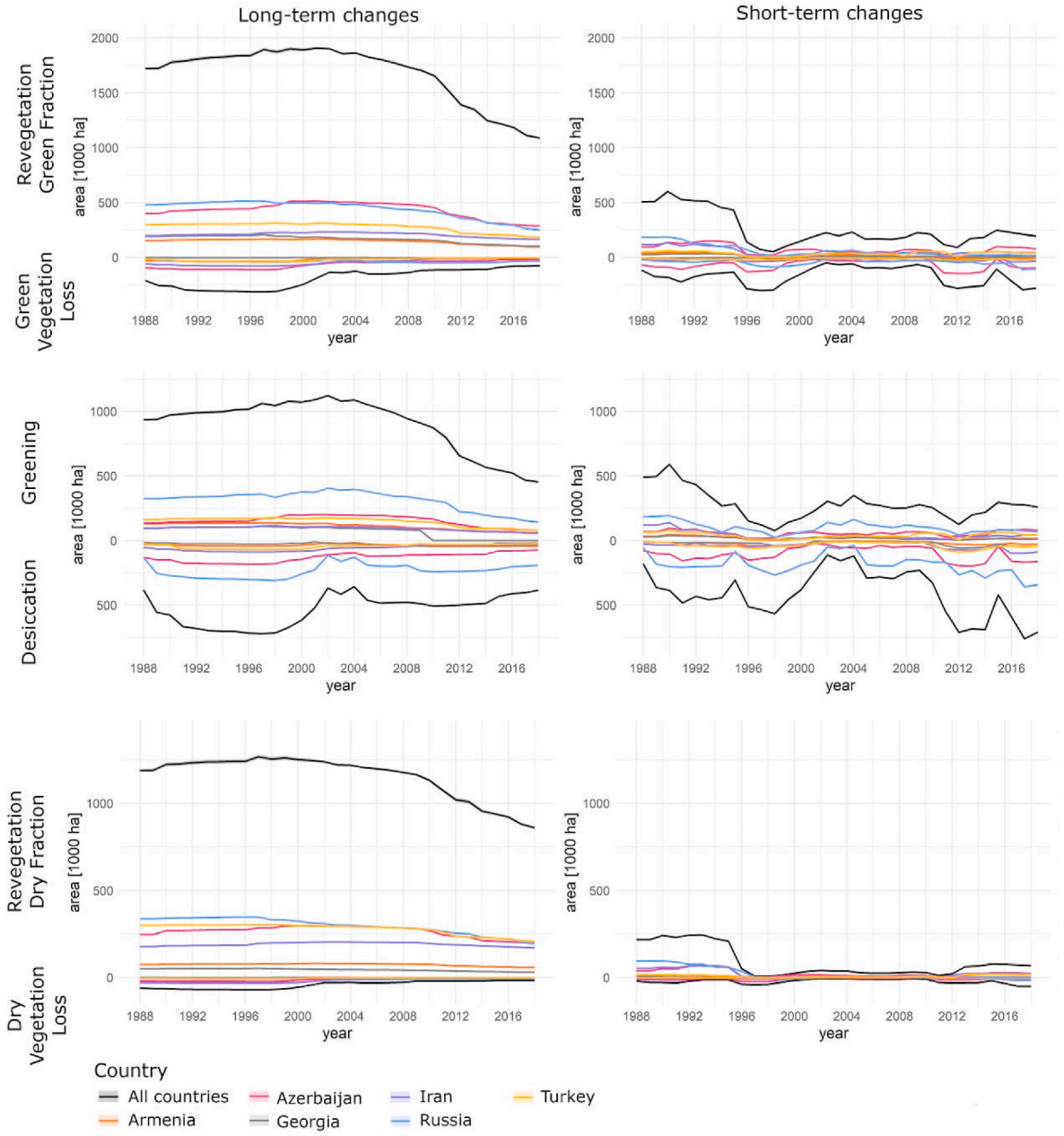

Fig. 6. Adjusted total area of revegetation green fraction, greening, revegetation dry fraction, green vegetation loss, desiccation, and dry vegetation loss mapped separately for long-term and short-term changes at the country level (values of the area adjustment coefficient are small, thus the shaded ribbons representing uncertainty are visible only for the 'All countries' category).

SPEI3 or livestock alone. The exception was in Krasnodar, Chechnya, Stavropol, and Dagestan regions in Russia, where integrating both factors improved explanatory power of the models (Table SA3-9).

3.5. *Changes in grassland vegetation cover at field scale*

Negative and positive changes in grassland vegetation cover often occurred in close proximity in the three analyzed grazing sites (Fig. 7). In the Pontic-Caspian steppe site (Fig. 7, region 1) we detected many large, irregular patches of desiccation, greening, and green vegetation loosely corresponding to the shepherd camps' location. There were few changes in vegetation cover in the 1980s and 1990s, moderate positive change in the 2000s, and intensified vegetation loss since 2005. Winter grazing sites in the Shirvain plain (Fig. 7, region 2) had compacted patches of revegetation of green and dry fractions near the Mughan Salyan Canal, and green vegetation loss and desiccation further away from it. Some of the latter changes had geometric footprints, suggesting that they reflect land management actions. Temporal development of changes in vegetation cover differed among the analyzed campsites in Shirvain plain suggesting site-specific changes, paired with widespread revegetation in the late 2000s. Changes in vegetation cover in the Kaçkar Mountains (Fig. 7, region 3) were limited to small patches of desiccation and greening located afar from the camps.

We observed no relationship between vegetation change pathways and the three distance zones. For example, we did not find higher probability of green vegetation loss nearer the camps. However, we did find more widespread vegetation changes in the sites in Russia and Azerbaijan after the 2000s, including more abundant negative changes.

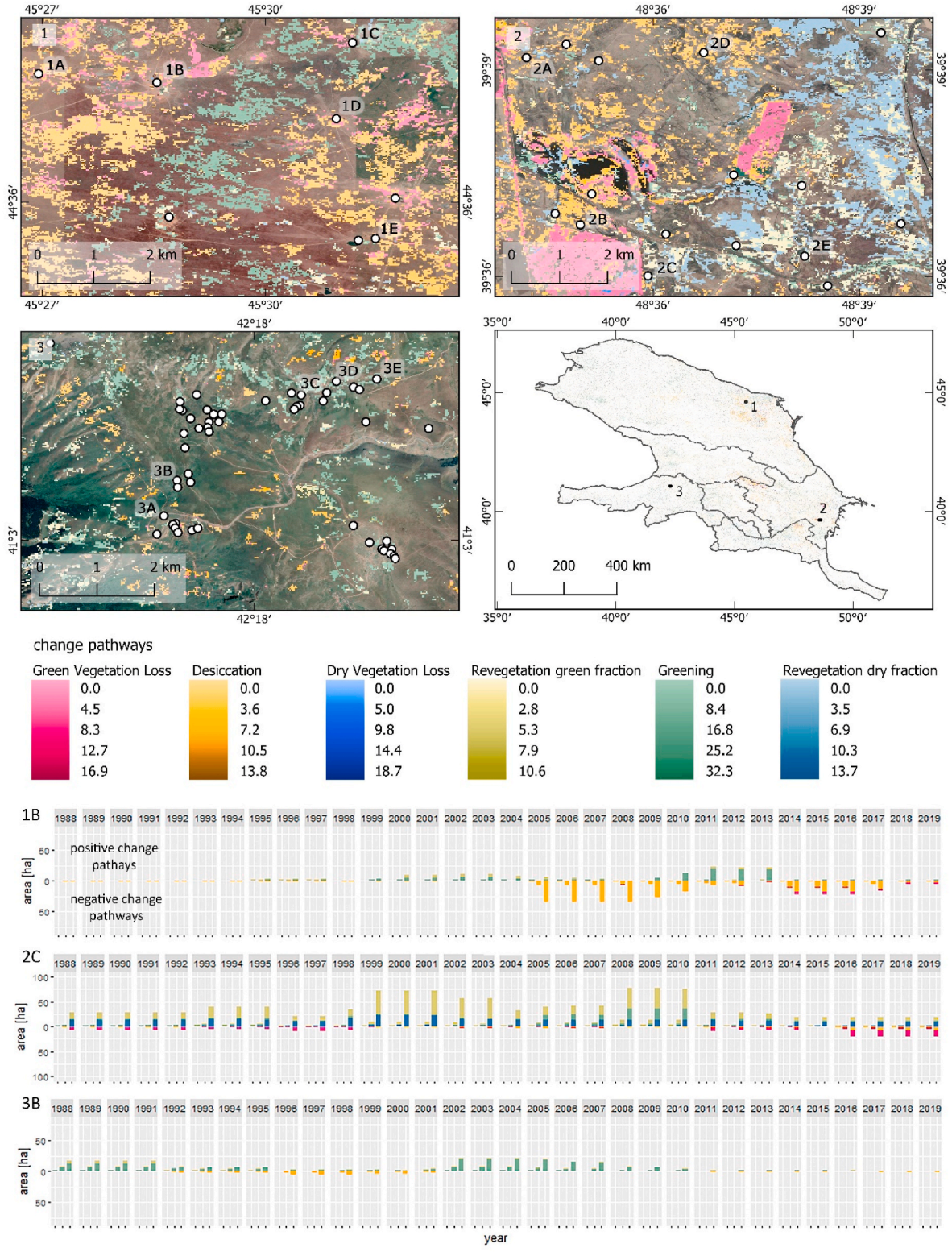

Fig. 7. Changes in grassland vegetation cover in 2018 (both short- and long-term changes) in: 1) Pontic Caspian steppe in Russia (winter grazing); 2) shrub desert steppe on Shirvain plain in Azerbaijan (winter grazing); and 3) in The Kaçkar Mountains in Turkey (summer grazing). Dots represent active shepherds' camps and enclosures (background: Google Earth). Below, three selected examples of area of positive and negative changes in grassland vegetation between 1988 and 2019 showed within three distances (0-250-m, 250-500-m, and 500–1,000-m, for left, center and right bar for each annual panel, respectively) centered at selected shepherds' camps. Please mind the different y-range in the plot 2C. Plots for the remaining marked camps in Figures SA16, SA17 and SA18.

4. Discussion

Mapping and monitoring changes in grassland vegetation cover is essential to understand grasslands dynamics and thus to support global ecosystem monitoring and sustainable land management. Unfortunately, grassland ecosystems lack the routine monitoring with medium-resolution satellite imagery that is standard, for example, for forests. Here, we adapted Cumulative Endmember Fractions (Lewińska et al., 2020) for the first time to analyze Landsat data and mapped short- and long-term negative and positive changes in grassland ground cover at 30-m resolution across the Caucasus. We found ample short- (3–9 years) and long-term (≥10 years) changes, both negative and positive, in grassland vegetation cover from 1987 to 2019. Furthermore, we found statistically significant relationship between green vegetation Cumulative Endmember Fraction and SPEI3 at regional level in Armenia, and green vegetation and small livestock numbers in Azerbaijan. The medium-resolution of the Landsat data makes our approach relevant for land management because vegetation dynamics of individual fields and pastures can be captured, as we demonstrated in three test sites.

4.1. Landsat based Cumulative Endmember Fractions

Availability of the clear-sky Landsat observations is often restricted, especially in the early years of the Landsat record (Wulder et al., 2016). Here, we applied the Whittaker filter to predict missing monthly composites, and it performed very well. Previous studies applied the Whittaker filter to fill gaps in MERIS and MODIS dense time series (Atkinson et al., 2012; Kandasamy et al., 2013), or annual values for Landsat (Study et al., 2020), but we were the first, to the best of our knowledge, to fill missing monthly Landsat values. Our predicting missing monthly observations had low to moderate error (Supplement B.1.), with a linear relation between number of missing data and RMSE of the fit (Figure SB4). The highest prediction errors occurred in mountain grasslands, most likely due to snow and more frequent cloud cover (Wilson and Jetz, 2016). Neither the accuracy of vegetation change detection, nor of vegetation change pathways were affected by low Landsat data availability in 2003 (due to SLC failure in Landsat 7 (Andréfouët et al., 2003)) (Figure SB1), or 2012 (due to several technical issues of Landsat 5).

4.2. Changes in grassland vegetation cover in the Caucasus Ecoregion

We found highly dynamic spatial and temporal pattern of changes in grassland vegetation cover in the Caucasus Ecoregion. Almost 45% of grasslands experienced at least one change in grassland green vegetation productivity or ground cover composition between 1987 and 2019, with many areas experiencing more than one change episode. This is in line with other studies that mapped up to four trend breakpoints from 1981 to 2008 based on 8-km GIMMS NDVI time series data in the region (de Jong et al., 2012), or ecosystem turning points between 1982 and 2011 (Horion et al., 2016). We identified long-term positive vegetation changes especially in the Kaçkar Mountains in Turkey, and in the Greater and Lesser Caucasus Mountains, similar to other studies (e.g., de Jong et al., 2012; Horion et al., 2016; Vinogradova and Gracheva, 2018). These positive changes are likely due to pasture abandonment stemming from outmigration (Radvanyi and Muduyev, 2007; Vinogradova and Gracheva, 2018), and to climate change (Gao et al., 2016), which often boost vegetation growth at high elevations (Jolly et al., 2005). Moreover, 2001–2013 gains in evapotranspiration and greenness in Armenia and central Azerbaijan mapped by de Beurs et al. (2015) coincide with greening change pathways in our time series during those years. Extensive and repetitive green vegetation loss and desiccation pathways in the Caspian Lowlands, Gobustan, and around the Mingachevir Reservoir also agree with other studies (de Beurs et al., 2015; de Jong et al., 2012) including our own previous MODIS based analysis (Lewińska et al., 2020), as well as local reports of increased land-use pressure (NACRES, 2013; Shatberashvili et al., 2015), and salinization (UNEP, 2011). More widespread short-term negative change pathways in late 1990s in Azerbaijan and the Iranian part of the Caucasus may have been due to regional drought conditions (Shayanmehr et al., 2020). Furthermore abrupt decline in short-term positive change pathways in Azerbaijan and Georgia around 1996 coincide with the implementation of national land reforms (Hartvigsen, 2013) and the end of the first war in Nagorno-Karabakh, which affected agricultural production in Azerbaijan in the early 1990s (Neudert, 2015).

In the northern Caucasus, we found widespread long-term positive changes in grassland vegetation cover, which partially align with 1999–2015 LAI trends (Munier et al., 2018) and are most likely due to the dramatic decrease in livestock numbers during the 1980s (Didebulidze and Plachtd, 2002; Smelansky and Tishkov, 2012). Lower grazing pressure allowed the steppe to recover, which in turn triggered an increase in grassland fires (Dubinin et al., 2010). This matches the 1996–2002 increase in short-term desiccation and green vegetation loss, and 2003–2011 short-term greening that we found in the northern Caucasus. The change in the fire regime due to biomass accumulation may be the reason for the almost complete cessation of short-term revegetation of green and dry fractions after 1996. Our results in the northern Caucasus differ from vegetation indices based trends in de Beurs et al. (2015) and de Jong et al. (2012), but we suggest that these disparities are due to different analytical approaches, variation in the length of the time series that were analyzed, different spatial resolution of the satellite data, and the fact that we analyzed only grasslands. Finally, the regional decrease in Tasseled Cap greenness and increase in brightness identified by de Beurs et al. (2015) matches our hotspots of desiccation and green vegetation loss pathways.

We found that the area of positive changes in vegetation cover in the Caucasus declined over time. While the decline of long-term positive pathways in the most recent years is due to our definition of long-term change, short-term changes did not compensate for the drop in long-term changes. Moreover, the increase in the area of negative change pathways since 2011 could be related to increasing degradation pressure (Patriche et al., 2021). Compared to our prior MODIS-based analyses (Lewińska et al., 2020), we found a lower area subjected to negative change pathways for 2002–2018, but the temporal trends were similar. The difference in area is mostly due to application of stricter threshold for change detection (20% vs. 10%), and the medium-resolution Landsat data.

Overall, our vegetation change detection had low annual commission error, but a somewhat higher omission error (Table SA2). That is opposite of what is typical for LandTrendr detection of forest disturbance, where commission errors are typically higher (Cohen et al., 2018, 2020). However, compared to grasslands, forests have less natural intra-annual variability, whereas their spectral change caused by disturbance typically is greater and lasts over several years, making detection easier. Finally, compared with other studies on grasslands done using LandTrendr (e.g., Dara et al., 2020), we mapped also the shortest and most subtle definition of change, which increased the complexity of the analysis, thus the probability for errors.

4.3. Effects of SPEI3 and livestock on the green vegetation Cumulative Endmember Fraction

The pixel-wise correlation between green vegetation Cumulative Endmember Fraction and SPEI3 was mostly insignificant in the Caucasus. This matches other studies (Ivits et al., 2016; Kamali and Khosravi, 2020), and is unlikely to be due to time lags because vegetation in the Caucasus has moderate to good resistance and resilience to short-term drought and temperature anomalies (De Keersmaecker et al., 2015; Ivits et al., 2016). We found only in grasslands at higher elevations that green vegetation was significantly correlated with SPEI3, which could be an effect of diminished anthropogenic pressure due to the ongoing outmigration from the mountain regions and pasture abandonment

(Radvanyi and Muduyev, 2007; Vinogradova and Gracheva, 2018), combined with better vegetation growth conditions at higher elevations due to climate change (Jolly et al., 2005). The positive relation between green vegetation Cumulative Endmember Fraction and SPEI3 in Azerbaijan west of the Mingachevir Reservoir suggests that this region, which was prior to 1991 a traditional winter pasture for herders from Georgia (Neudert, 2015), is not used as much anymore.

The relation between green vegetation Cumulative Endmember Fraction and small livestock numbers and SPEI3 on national and regional level varied across the Caucasus, but our models found only a few significant relationships between green vegetation Cumulative Endmember Fraction and SPEI3 or livestock. SPEI was only clearly related to green vegetation in Armenia, but not in the other countries. Livestock was overall significantly positively associated with green vegetation in regions where grazing occurs in steppe vegetation, opposite to what we expected, but only moderately so. In provinces where mountain grasslands dominate and grazing pressure is low, SPEI3 had the greatest predictive power.

The low explanatory power of our models does not mean that climatic conditions and livestock numbers do not determine the amount of green vegetation in the region. Instead, we suggest that the reason why our models were only mildly successful in explaining the changes in green vegetation is that the relevant processes, especially grazing and livestock management, happen at fine scales. Our livestock data, which was only available for regions, did not capture these fine-scale processes, and while the SPEI3 data had higher spatial resolution, they alone could not capture the interactive effects of livestock and climate. Moreover, there were some discrepancies between where animals were registered and where they grazed, and livestock population estimates are biased low because the census is conducted in winter when the population reaches its annual low point (Leeuw et al., 2019). Furthermore, model performances could have been lower in regions that employ fallowing (Yin et al., 2018), selective resting (Neudert, 2015), or grazing on harvested fields. Finally, beside sheep and goats, cows, horses, mules and camels are also grazed in the Caucasus (Neudert, 2015; Neudert et al., 2019; Smelansky and Tishkov, 2012), and the proportion of big cattle grazed outdoors and being kept indoors varies among countries and regions (Didebulidze and Plachtd, 2002). Consequently, without detailed information on herd structures, including big cattle into our models would introduce additional uncertainty, especially when measures that convert all livestock species to 'sheep units' are not adjusted for differences in grazing effects due to pinching height or stomping, which are important in steppe ecosystems (Smelansky and Tishkov, 2012). These other issues aside though, we attribute the limited explanatory power of our models mainly to the coarse scale of the livestock data, and the high spatial heterogeneity of green vegetation patterns that we detected thanks to Landsat's 30-m resolution supports that assertion.

4.4. Changes in grassland vegetation cover at field scale

We found great heterogeneity in the spatial and temporal patterns of vegetation change in proximity of the shepherds' camps in all three sites. The lack of expected concentric patterns of vegetation change around camps is likely due to camp organization, herding practices, and land management. When we digitized the camps, we noted remains of abandoned old buildings and animal enclosures dispersed throughout the Shirvain plains sites. Throughout the Caucasus, camps were sometimes abandoned due to limited building maintenance during the 1990s, and due to the current land tenure system in which investment into building assets often depends on the length of a lease (Neudert, 2015; Neudert and Allahverdiyeva, 2009). In Pontic Caspian steppe, camps' locations remained stable but in only some cases was there severe degradation and desertification nearby. Finally in Turkey, complex topography and collective character of camps comprising many small enclosures and huts or tents complicated the distance-based analyses. Overall though, our field scale results showed a high level of spatio-temporal heterogeneity of vegetation change, which arises from complexity of local environmental conditions, land management and land use history, with many meadows being transformed into pastures from croplands, thus fostering different species composition (Belonovskaya et al., 2016; Vinogradova and Gracheva, 2018). This highlights importance of mapping grassland dynamics with 30-m satellite data, instead of coarse-resolution data.

5. Conclusions

Reliable monitoring of changes in vegetation cover in grasslands is crucial for accurate and sustainable land management and thus ultimately for achieving Land Degradation Neutrality goals and curbing climate change. Here, we developed a novel way to map changes in grassland to monitor both long- and short-term, as well as positive and negative changes in grassland vegetation at 30-m resolution based on the complete Landsat archive. Our approach combining existing algorithms and methods worked well and provided unique temporal and spatial information on vegetation dynamics across the Caucasus Ecoregion since the mid-1980s. Importantly, we were able to distinguish among six change pathways, providing better insight into the types of changes that occurred. Interestingly though, the variability in green vegetation Cumulative Endmember Fraction was generally not well explained by either meteorological conditions or small livestock numbers, most likely because the spatial detail of the vegetation changes captured by Landsat is due to fine-scale differences in grazing that are not captured by coarse livestock data.

To the best of our knowledge our analysis is the first pan-Caucasus study of vegetation change since the Soviet era in the mid-1980s at 30-m resolution, and one of only a handful of studies to analyze grassland conditions for a large area based on the full Landsat time series. As such, our results offer new insights into vegetation change processes. Maybe more importantly, our new approach is globally applicable yet management-relevant at local scales, as its physically-based origin provides a strong quantitative foundation to study grassland change processes.

Declaration of competing interest

The authors declare that they have no known competing financial interests or personal relationships that could have appeared to influence the work reported in this paper.

Acknowledgements

We gratefully acknowledge support from the Land Cover and Land Use Change (LCLUC) Program of the National Aeronautic Space Administration (NASA), Grants 80NSSC18K0316 and 80NSSC18K0343. We thank E. Razenkova and A. Rizayeva for their support, and D. Schkirkie for proofreading. We also express our gratitude to D. Kong for sharing his Whittaker codes openly. The authors want to thank four anonymous reviewers whose comments improved the quality of the paper.

Appendix A. Supplementary data

Supplementary data to this article can be found online at https://doi.org/10.1016/j.srs.2021.100035.

Data availability

Vegetation change maps are available at http://silvis.forest.wisc.edu/data2/vegetation-change-grasslands-caucasus/.

References

Abatzoglou, J.T., Dobrowski, S.Z., Parks, S.A., Hegewisch, K.C., 2018. TerraClimate, a high-resolution global dataset of monthly climate and climatic water balance from 1958-2015. Sci. Data 5, 1–12. https://doi.org/10.1038/sdata.2017.191.

Ali, I., Cawkwell, F., Dwyer, E., Barrett, B., Green, S., 2016. Satellite remote sensing of grasslands: from observation to management. J. Plant Ecol. 9, 649–671. https://doi.org/10.1093/jpe/rtw005.

Andréfouët, S., Bindschadler, R., Brown De Colstoun, E.C., Choate, M., Chomentowski, W., Christopherson, J., Doorn, B., Hall, D.K., Holifield, C., Howard, S., Kranenburg, C., Lee, S., Masek, J.B., Moran, M., Mueller-Karger, F., Ohlen, D., Palandro, D., Price, J., Qi, J., Reed, B.C., Samek, J., Scaramuzza, P., Skole, D., Schott, J., Storey, J., Thome, K., Torres-Pulliza, D., Vogelmann, J., Williams, D.L., Woodcock, C., Wylie, B., 2003. Preliminary assessment of the value of landsat 7 ETM+ data following scan line corrector malfunction. Science (80-.) 1–86.

Atkinson, P.M., Jeganathan, C., Dash, J., Atzberger, C., 2012. Inter-comparison of four models for smoothing satellite sensor time-series data to estimate vegetation phenology. Remote Sens. Environ. 123, 400–417. https://doi.org/10.1016/j.rse.2012.04.001.

Belonovskaya, E., Gracheva, R., Shorkunov, I., Vinogradova, V., 2016. Grasslands of intermontane basins of Central Caucasus: land use legacies and present-day state. Hacquetia 15, 37–47. https://doi.org/10.1515/hacq-2016-0016.

Bleyhl, B., Baumann, M., Griffiths, P., Heidelberg, A., Manvelyan, K., Radeloff, V.C., Zazanashvili, N., Kuemmerle, T., 2017. Assessing landscape connectivity for large mammals in the Caucasus using Landsat 8 seasonal image composites. Remote Sens. Environ. 193, 193–203. https://doi.org/10.1016/j.rse.2017.03.001.

Bleyhl, B., Arakelyan, M., Askerov, E., Bluhm, H., Gavashelishvili, A., Ghasabian, M., Ghoddousi, A., Heidelberg, A., Khorozyan, I., Malkhasyan, A., Manvelyan, K., 2019. Assessing Niche Overlap between Domestic and Threatened Wild Sheep to Identify Conservation Priority Areas 129–141. https://doi.org/10.1111/ddi.12839.

Buchner, J., Yin, H., Frantz, D., Kuemmerle, T., Bleyhl, B., Bakuradze, T., Elizbarashvili, N., Komarova, A., Lewińska, K.E., Rizayeva, A., Sayadyan, H., Tan, B., Tepanosyan, G., Zazanashvili, N., Radeloff, V.C., 2020. Land-cover change in the Caucasus Mountains since 1987 based on topographic correction of multi-temporal Landsat composites. Remote Sens. Environ. 248 https://doi.org/10.1016/j.rse.2020.111967.

Buenemann, M., Martius, C., Jones, J.W., Herrmann, S.M., Klein, D., Mulligan, M., Reed, M.S., Winslow, M., Washington-Allen, R.A., Lal, R., Ojima, D., 2011. Integrative geospatial approaches for the comprehensive monitoring and assessment of land management sustainability: rationale, Potentials, and Characteristics. Land Degrad. Dev. 22, 226–239. https://doi.org/10.1002/ldr.1074.

Chen, J., Jönsson, P., Tamura, M., Gu, Z., Matsushita, B., Eklundh, L., 2004. A simple method for reconstructing a high-quality NDVI time-series data set based on the Savitzky-Golay filter. Remote Sens. Environ. 91, 332–344. https://doi.org/10.1016/j.rse.2004.03.014.

Cherlet, M., Hutchinson, C., Reynolds, J., Hill, J., Sommer, S., von Maltitz, G. (Eds.), 2018. World Atlas of Desertification. Publication Office of the European Union, Luxembourg. https://doi.org/10.2760/9205.

Cohen, W.B., Yang, Z., Healey, S.P., Kennedy, R.E., Gorelick, N., 2018. A LandTrendr multispectral ensemble for forest disturbance detection. Remote Sens. Environ. 205, 131–140. https://doi.org/10.1016/j.rse.2017.11.015.

Cohen, W.B., Healey, S.P., Yang, Z., Zhu, Z., Gorelick, N., 2020. Diversity of Algorithm and Spectral Band Inputs Improves Landsat Monitoring of Forest Disturbance 1–15. https://doi.org/10.3390/rs12101673.

Cowie, A.L., Orr, B.J., Castillo Sanchez, V.M., Chasek, P., Crossman, N.D., Erlewein, A., Louwagie, G., Maron, M., Metternicht, G.I., Minelli, S., Tengberg, A.E., Walter, S., Welton, S., 2018. Land in balance: the scientific conceptual framework for Land Degradation Neutrality. Environ. Sci. Pol. 79, 25–35. https://doi.org/10.1016/j.envsci.2017.10.011.

Dara, A., Baumann, M., Freitag, M., Hölzel, N., Hostert, P., Kamp, J., Müller, D., Prishchepov, A.V., Kuemmerle, T., 2020. Annual Landsat time series reveal post-Soviet changes in grazing pressure. Remote Sens. Environ. 239, 111667. https://doi.org/10.1016/j.rse.2020.111667.

de Beurs, K.M., Henebry, G.M., Owsley, B.C., Sokolik, I., 2015. Using multiple remote sensing perspectives to identify and attribute land surface dynamics in Central Asia 2001-2013. Remote Sens. Environ. 170, 48–61. https://doi.org/10.1016/j.rse.2015.08.018.

de Jong, R., Verbesselt, J., Schaepman, M.E., de Bruin, S., 2012. Trend changes in global greening and browning: contribution of short-term trends to longer-term change. Global Change Biol. 18, 642–655. https://doi.org/10.1111/j.1365-2486.2011.02578.x.

De Keersmaecker, W., Lhermitte, S., Tits, L., Honnay, O., 2015. A model quantifying global vegetation resistance and resilience to short-term climate anomalies and their relationship with vegetation cover. Global Change Biol. 20, 2149–2161. https://doi.org/10.1111/geb.12279.

Didebulidze, A., Plachtd, H., 2002. Nature Conservation Aspects of Pastoral Farming in Georgia.

Dubinin, M., Potapov, P., Lushchekina, A., Radeloff, V.C., 2010. Reconstructing long time series of burned areas in arid grasslands of southern Russia by satellite remote sensing. Remote Sens. Environ. 114, 1638–1648. https://doi.org/10.1016/j.rse.2010.02.010.

Eilers, P.H.C., 2003. A perfect smoother. Anal. Chem. 75, 3631–3636. https://doi.org/10.1021/ac034173t.

Elizbarashvili, M., Elizbarashvili, E., Tatishvili, M., Elizbarashvili, S., Meskhia, R., Kutaladze, N., King, L., Keggenhoff, I., Khardziani, T., 2017. Georgian climate change under global warming conditions. Ann. Agrar. Sci. 15, 17–25. https://doi.org/10.1016/j.aasci.2017.02.001.

Elmore, A.J., Mustard, J.F., Manning, S.J., Lobell, D.B., 2000. Quantifying vegetation change in semiarid environments: precision and accuracy of spectral mixture analysis and the normalized difference vegetation index. Remote Sens. Environ. 102, 87–102. https://doi.org/10.1016/S0034-4257(00)00100-0.

FAO, 2005. Grasslands of the World. Food and Agricultural Organization of the United Nations, Rome, 2005.

FAO, 2020. FAOSTAT [WWW Document]. FAOSTAT. URL. http://www.fao.org/faostat/en/#data.

Foga, S., Scaramuzza, P.L., Guo, S., Zhu, Z., Dilley, R.D., Beckmann, T., Schmidt, G.L., Dwyer, J.L., Joseph Hughes, M., Laue, B., 2017. Cloud detection algorithm comparison and validation for operational Landsat data products. Remote Sens. Environ. 194, 379–390. https://doi.org/10.1016/j.rse.2017.03.026.

Gao, F., Masek, J., Schwaller, M., Hall, F., 2006. On the blending of the MODIS and landsat ETM + surface Reflectance : Predicting daily landsat surface reflectanc. IEEE Trans. Geosci. Rem. Sens. 44, 2207–2218. https://doi.org/10.1109/TGRS.2006.872081.

Gao, F., Hilker, T., Zhu, X., Anderson, M., Masek, J., Wang, P., Yang, Y., 2015. Fusing landsat and MODIS data for vegetation monitoring. IEEE Geosci. Remote Sens. Mag. 3, 47–60. https://doi.org/10.1109/MGRS.2015.2434351.

Gao, Q., Zhu, W., Schwartz, M.W., Ganjurjav, H., Wan, Y., 2016. Climatic change controls productivity variation in global grasslands. Nat. Publ. Gr. 1–10. https://doi.org/10.1038/srep26958.

Gorelick, N., Hancher, M., Dixon, M., Ilyushchenko, S., Thau, D., Moore, R., 2017. Google Earth engine: planetary-scale geospatial analysis for everyone. Remote Sens. Environ. 202, 18–27. https://doi.org/10.1016/j.rse.2017.06.031.

Griffiths, P., Nendel, C., Pickert, J., Hostert, P., 2020. Towards national-scale characterization of grassland use intensity from integrated Sentinel-2 and Landsat time series. Remote Sens. Environ. 238, 111124. https://doi.org/10.1016/j.rse.2019.03.017.

Hartvigsen, M., 2013. Land Reform in Central and Eastern Europe after 1989 and its Outcome in the Form of Farm Structures and Land Fragmentation.

Hobi, M.L., Dubinin, M., Graham, C.H., Coops, N.C., Clayton, M.K., Pidgeon, A.M., Radeloff, V.C., 2017. A comparison of Dynamic Habitat Indices derived from different MODIS products as predictors of avian species richness. Remote Sens. Environ. 195, 142–152. https://doi.org/10.1016/j.rse.2017.04.018.

Holland, E.C., 2016. Economic development and subsidies in the north Caucasus. Probl. Post-Communism 63, 50–61. https://doi.org/10.1080/10758216.2015.1067750.

Horion, S., Cornet, Y., Erpicum, M., Tychon, B., 2012. Studying interactions between climate variability and vegetation dynamic using a phenology based approach. Int. J. Appl. Earth Obs. Geoinf. 20, 20–32. https://doi.org/10.1016/j.jag.2011.12.010.

Horion, S., Prishchepov, A.V., Verbesselt, J., de Beurs, K., Tagesson, T., Fensholt, R., 2016. Revealing turning points in ecosystem functioning over the Northern Eurasian agricultural frontier. Global Change Biol. 22, 2801–2817. https://doi.org/10.1111/gcb.13267.

Hostert, P., Röder, A., Hill, J., 2003. Coupling spectral unmixing and trend analysis for monitoring of long-term vegetation dynamics in Mediterranean rangelands. Remote Sens. Environ. 87, 183–197. https://doi.org/10.1016/s0034-4257(03)00145-7.

Hovsepyan, R., 2015. On the agriculture and vegetal food economy of Kura-Araxes culture in the South Caucasus. Paleorient 41, 69–82. https://doi.org/10.3406/paleo.2015.5656.

IPBES, 2018. The IPBES Assessment Report on Land Degradation and Restoration. Companion to Environmental Studies, Bonn, Germany. https://doi.org/10.4324/9781315640051-105.

IPCC, 2019. Special Report on Climate Change and Land. Ipcc.

Ivits, E., Horion, S., Erhard, M., Fensholt, R., 2016. Assessing European ecosystem stability to drought in the vegetation growing season. Global Ecol. Biogeogr. 25, 1131–1143. https://doi.org/10.1111/geb.12472.

Jolly, W.M., Dobbertin, M., Zimmermann, N.E., Reichstein, M., 2005. Divergent vegetation growth responses to the 2003 heat wave in the Swiss Alps. Geophys. Res. Lett. 32, 2–5. https://doi.org/10.1029/2005GL023252.

Kamali, A., Khosravi, M., 2020. Spatial–temporal analysis of net primary production (NPP) and its relationship with climatic factors in Iran. Environ. Monit. Assess. 192 https://doi.org/10.1007/s10661-020-08667-7.

Kandasamy, S., Baret, F., Verger, A., Neveux, P., Weiss, M., 2013. A comparison of methods for smoothing and gap filling time series of remote sensing observations & ndash; application to MODIS LAI products. Biogeosciences 10, 4055–4071. https://doi.org/10.5194/bg-10-4055-2013.

Kennedy, R.E., Yang, Z., Cohen, W.B., 2010. Detecting trends in forest disturbance and recovery using yearly Landsat time series: 1. LandTrendr - temporal segmentation algorithms. Remote Sens. Environ. 114, 2897–2910. https://doi.org/10.3899/jrheum.111106.

Kennedy, R.E., Yang, Z., Gorelick, N., Braaten, J., Cavalcante, L., Cohen, W.B., Healey, S., 2018. Implementation of the LandTrendr algorithm on Google Earth engine. Rem. Sens. 10, 1–10. https://doi.org/10.3390/rs10050691.

Kong, D., Zhang, Y., Gu, X., Wang, D., 2019. A robust method for reconstructing global MODIS EVI time series on the Google Earth Engine. ISPRS J. Photogrammetry Remote Sens. 155, 13–24. https://doi.org/10.1016/j.isprsjprs.2019.06.014.

Leeuw, J. De, Rizayeva, A., Namazov, E., Bayramov, E., Marshall, M.T., Etzold, J., Neudert, R., 2019. Application of the MODIS MOD 17 Net Primary Production product in grassland carrying capacity assessment. Int. J. Appl. Earth Obs. Geoinf. 78, 66–76. https://doi.org/10.1016/j.jag.2018.09.014.

Lewińska, K.E., Hostert, P., Buchner, J., Bleyhl, B., Radeloff, V.C., 2020. Short-term vegetation loss versus decadal degradation of grasslands in the Caucasus based on

Cumulative Endmember Fractions. Remote Sens. Environ. 248 https://doi.org/10.1016/j.rse.2020.111969.
Marchese, C., 2015. Biodiversity hotspots : a shortcut for a more complicated concept. Glob. Ecol. Conserv. 3, 297–309. https://doi.org/10.1016/j.gecco.2014.12.008.
Masek, J.G., Vermote, E.F., Saleous, N.E., Wolfe, R., Hall, F.G., Huemmrich, K.F., Gao, F., Kutler, J., Lim, T.K., 2006. A landsat surface reflectance dataset for North America, 1990-2000. Geosci. Rem. Sens. Lett. IEEE 3, 68–72. https://doi.org/10.1109/LGRS.2005.857030.
Masiliunas, D., Tsendbazar, N., Herold, M., Lesiv, M., Buchhorn, M., Verbesselt, J., 2021. Global land characterisation using land cover fractions at 100 m resolution. Remote Sens. Environ. 259 https://doi.org/10.1016/j.rse.2021.112409.
Miao, L., Sun, Z., Müller, D., Ren, Y., Schierhorn, F., 2021. Grassland Greening on the Mongolian Plateau Despite Higher Grazing Intensity 792–802. https://doi.org/10.1002/ldr.3767.
Ministers of Azerbaijan, Cabinet, 2008. Grazing Land Action Plan (2011-2015) of the State Programme on Poverty Reduction and Sustainable Development of the Republic of Azerbaijan (2008-2015). Report of the Sustainable Management of Pastures Project TCP/AZE/3302 (D). Baku, Azerbaijan.
Munier, S., Carrer, D., Planque, C., Camacho, F., 2018. Satellite Leaf Area Index : Global Scale Analysis of the Tendencies Per Vegetation Type over the Last 17 Years 1–25. https://doi.org/10.3390/rs10030424.
NACRES, 2013. Assessment of Pastures in Vashlovani National Park. Tibilisi.
Neely, C., Bunning, S., Wilkes, A., 2009. Review of evidence on drylands pastoral systems and climate change. L. Water Discuss. Papp. 8.
Neudert, R., 2015. Is individualized rangeland lease institutionally incompatible with mobile pastoralism? - a case study from post-socialist Azerbaijan. Hum. Ecol. 43, 785–798. https://doi.org/10.1007/s10745-015-9792-7.
Neudert, R., Allahverdiyeva, N.K., 2009. Economic performance of transhumant sheep farming in Azerbaijan and prospects for its future development. South Cauc. Ann. Agrar. Sci. 7, 153–157.
Neudert, R., Salzer, A., Allahverdiyeva, N., Etzold, J., Beckmann, V., 2019. Archetypes of common village pasture problems in the south Caucasus: insights from comparative case studies in Georgia and Azerbaijan. Ecol. Soc. 24 https://doi.org/10.5751/ES-10921-240305.
Olofsson, P., Foody, G.M., Herold, M., Stehman, S.V., Woodcock, C.E., Wulder, M.A., 2014. Good practices for estimating area and assessing accuracy of land change. Remote Sens. Environ. 148, 42–57. https://doi.org/10.1016/j.rse.2014.02.015.
O'Loughlin, J., Kolossov, V., Radvanyi, J., 2007. The Caucasus in a time of conflict, demographic transition, and economic change. Eurasian Geogr. Econ. 48, 135–156. https://doi.org/10.2747/1538-7216.48.2.135.
O'Mara, F.P., 2012. The role of grasslands in food security and climate change. Ann. Bot. 110, 1263–1270. https://doi.org/10.1093/aob/mcs209.
Patriche, C., Borrelli, P., Panagos, P., Roșca, B., Pr, R., Dumitras, M., Bandoc, G., 2021. Arable lands under the pressure of multiple land degradation processes . A global perspective. Environ. Res. 194 https://doi.org/10.1016/j.envres.2020.110697.
Radvanyi, J., Muduyev, S.S., 2007. Challenges facing the mountain peoples of the Caucasus. Eurasian Geogr. Econ. 48, 157–177. https://doi.org/10.2747/1538-7216.48.2.157.
Reed, B.C., Brown, J., VanderZee, D., Loveland, T., Merchant, J., Ohlen, D.O., 1994. Measuring phenological variability from satellite imagery. J. Veg. Sci. 5, 703–714.
Reed, M.S., Buenemann, M., Atlhopheng, J., Akhtar-Schuster, M., Bachmann, F., Bastin, G., Bigas, H., Chanda, R., Dougill, a J., Essahli, W., Evely, a C., Fleskens, L., Geeson, N., Glass, J.H., Hessel, R., Holden, J., Ioris, a a R., Kruger, B., Liniger, H.P., Mphinyane, W., Nainggolan, D., Perkins, J., Raymond, C.M., Ritsema, C.J., Schwilch, G., Sebego, R., Seely, M., Stringer, L.C., Thomas, R., Twomlow, S., Verzandvoort, S., 2011. Cross-scale monitoring and assessment of land degradation and sustainable land management: a methodological framework for knowledge management. Land Degrad. Dev. 22, 261–271. https://doi.org/10.1002/ldr.1087.
Reinermann, S., Asam, S., Kuenzer, C., 2020. Remote sensing of grassland production and management-A review. Rem. Sens. 12 https://doi.org/10.3390/rs12121949.
Roy, D.P., Kovalskyy, V., Zhang, H.K., Vermote, E.F., Yan, L., Kumar, S.S., Egorov, A., 2016. Characterization of Landsat-7 to Landsat-8 reflective wavelength and normalized difference vegetation index continuity. Remote Sens. Environ. 185, 57–70. https://doi.org/10.1016/j.rse.2015.12.024.
Schwieder, M., Leitão, P.J., da Cunha Bustamante, M.M., Ferreira, L.G., Rabe, A., Hostert, P., 2016. Mapping Brazilian savanna vegetation gradients with Landsat time series. Int. J. Appl. Earth Obs. Geoinf. 52, 361–370. https://doi.org/10.1016/j.jag.2016.06.019.
Shatberashvili, N., Rucevska, I., Jørstad, H., Artsivadze, K., Mehdiyev, B., Aliyev, M., Fayvush, G., Dzneladze, M., Jurek, M., Kirkfeldt, T., Semernya, L., 2015. Outlook on Climate Change Adaptation in the South Caucasus Mountains. United Nations Environment Programme, GRID-Arendal and Sustainable Caucasus, Nairobi. https://doi.org/10.13140/RG.2.1.4311.1287. Arendal and Tbilisi.
Shayanmehr, S., Henneberry, S.R., Sabouni, M.S., 2020. Drought , climate change , and dryland wheat yield response : an econometric approach. Int. J. Environ. Res. Publ. Health 17. https://doi.org/10.3390/ijerph17145264.
Smelansky, I.E., Tishkov, A.A., 2012. The steppe biome in Russia: ecosystem services , conservation status, and actual challenges. In: Eurasian Steppes. Ecological Problems and Livelihoods in a Changing World, pp. 45–101. https://doi.org/10.1007/978-94-007-3886-7.
Sonnenschein, R., Kuemmerle, T., Udelhoven, T., Stellmes, M., Hostert, P., 2011. Differences in Landsat-based trend analyses in drylands due to the choice of vegetation estimate. Remote Sens. Environ. 115, 1408–1420. https://doi.org/10.1016/j.rse.2011.01.021.
Stanimirova, R., Arévalo, P., Kaufmann, R.K., Maus, V., 2019. Sensitivity of global pasturelands to climate variation Earth ' s future. Earth's Futur. 7, 1353–1366. https://doi.org/10.1029/2019EF001316.
Stehman, S.V., 2014. Estimating area and map accuracy for stratified random sampling when the strata are different from the map classes. Int. J. Rem. Sens. 35, 4923–4929. https://doi.org/10.1080/01431161.2014.930207.
Study, A.C., Khanal, N., Matin, M.A., Uddin, K., Poortinga, A., 2020. A comparison of three temporal smoothing algorithms to improve land cover classification: a case study from Nepal. Rem. Sens. 12, 5–7. https://doi.org/10.3390/rs12182888.
Tepanosyan, G.H., Asmaryan, S.G., Muradyan, V.S., Saghatelyan, A.K., 2017. Mapping man-induced soil degradation in Armenia's high mountain pastures through remote sensing methods: a case study. Remote Sens. Appl. Soc. Environ. 8, 105–113. https://doi.org/10.1016/j.rsase.2017.08.006.
Tindall, D., Scarth, P., Schmidt, M., Muir, J., Trevithick, R., Denham, R., Pringle, M., Witte, C., 2012. The queensland ground cover monitoring program. In: Congress, I.S. P.R.S. (Ed.), International Archives of the Photogrammetry, Remote Sensing and Spatial Information Sciences, ISPRS CongressAt. Melbourne, Australia. Melbourne.
UNCCD, 1994. United Nations Convention to Combat Desertification in Those Countries Experiencing Serious Drought And/or Desertification. Particularly in Africa, Paris.
UNCCD, 2017a. UNCCD - ICCD/COP(13)/L.18 - the future strategic framework of the Convention - draft decision submitted by the. Chair of the Committee of the Whole, 16078, 1–9.
UNCCD, 2017b. Integration of Sustainable Development Goal 15 and Related Target 15.3 Which States: "To Combat Desertification, Restore Degraded Land and Soil, Including Land Affected by Desertification, Drought and Floods, and Strive to Achieve a Land Degradation-Neutr. Ordos, China. GE.19-10284(E).
UNEP, 2011. Caspian Sea State of the Environment. Encyclopedia of Environment and Society.
University of East Anglia Climatic Research Unit, Harris, I.C., Jones, P.D., 2017. CRU TS4.00: Climatic Research Unit (CRU) Time-Series (TS) version 4.00 of high-resolution gridded data of month-by-month variation in climate (Jan. 1901- Dec. 2015). https://doi.org/10.5285/edf8febfdaad48abb2cbaf7d7e846a86.
Verbesselt, J., Hyndman, R., Newnham, G., Culvenor, D., 2010. Detecting trend and seasonal changes in satellite image time series. Remote Sens. Environ. 114, 106–115. https://doi.org/10.1016/j.rse.2009.08.014.
Vermote, E., Justice, C., Claverie, M., Franch, B., 2016. Preliminary analysis of the performance of the Landsat 8/OLI land surface reflectance product. Remote Sens. Environ. 185, 46–56. https://doi.org/10.1016/j.rse.2016.04.008.
Vicente-serrano, S.M., 2007. Evaluating the Impact of Drought Using Remote Sensing in a Mediterranean , Semi-arid Region 173–208. https://doi.org/10.1007/s11069-006-0009-7.
Vicente-Serrano, S.M., Beguería, S., López-Moreno, J.I., 2010. A multiscalar drought index sensitive to global warming: the standardized precipitation evapotranspiration index. J. Clim. 23, 1696–1718. https://doi.org/10.1175/2009JCLI2909.1.
Vicente-Serrano, S.M., Beguería, S., Lorenzo-Lacruz, J., Camarero, J.J., López-Moreno, J. I., Azorin-Molina, C., Revuelto, J., Morán-Tejeda, E., Sanchez-Lorenzo, A., 2012. Performance of drought indices for ecological, agricultural, and hydrological applications. Earth Interact. 16 https://doi.org/10.1175/2012EI000434.1.
Vinogradova, V., Gracheva, R., 2018. Climate Change Effects on Mountain Regions Marginalized by Socio- Economic Transformation—The Case of North Caucasus Chapter. Springer International Publishing, pp. 79–90. https://doi.org/10.1007/978-3-319-59002-8.
Wang, X., Li, F., Gao, R., Luo, Y., Liu, T., 2014. Predicted NPP spatiotemporal variations in a semiarid steppe watershed for historical and trending climates. J. Arid Environ. 104, 67–79. https://doi.org/10.1016/j.jaridenv.2014.02.003.
Whittaker, E.T., 1922. On a new method of graduation. Proc. Edinb. Math. Soc. 41, 63–75. https://doi.org/10.1017/S0013091500077853.
Wiesmair, M., Feilhauer, H., Magiera, A., Otte, A., Waldhardt, R., 2016. Estimating vegetation cover from high-resolution satellite data to assess grassland degradation in the Georgian Caucasus. Mt. Res. Dev. 36, 56–65. https://doi.org/10.1659/MRD-JOURNAL-D-15-00064.1.
Wilson, A.M., Jetz, W., 2016. Remotely sensed high-resolution global cloud dynamics for predicting ecosystem and biodiversity distributions. PLoS Biol. 14, 1–20. https://doi.org/10.1371/journal.pbio.1002415.
Woodcock, C.E., Allen, R., Anderson, M., Belward, A., Bindschadler, R., Cohen, W., Gao, F., Goward, S.N., Helder, D., Helmer, E., Nemani, R., Oreopoulos, L., Schott, J., Thenkabail, P.S., Vermote, E.F., Vogelmann, J., Wulder, M.A., Wynne, R., 2008. Free access to landsat imagery. Science (80- 320, 1011–1012. https://doi.org/10.1126/science.320.5879.1011a.
Wulder, M.A., White, J.C., Loveland, T.R., Woodcock, C.E., Belward, A.S., Cohen, W.B., Fosnight, E.A., Shaw, J., Masek, J.G., Roy, D.P., 2016. The global Landsat archive: status, consolidation, and direction. Remote Sens. Environ. 185, 271–283. https://doi.org/10.1016/j.rse.2015.11.032.
Xie, Z., Phinn, S.R., Game, E.T., Pannell, D.J., Hobbs, R.J., Briggs, P.R., McDonald-Madden, E., 2019. Using Landsat observations (1988–2017) and Google Earth Engine to detect vegetation cover changes in rangelands - a first step towards identifying degraded lands for conservation. Remote Sens. Environ. 232, 111317. https://doi.org/10.1016/j.rse.2019.111317.
Yan, L., Roy, D.P., 2020. Spatially and temporally complete Landsat reflectance time series modelling: the fill-and-fit approach. Remote Sens. Environ. 241 https://doi.org/10.1016/j.rse.2020.111718.
Yin, H., Prishchepov, A.V., Kuemmerle, T., Bleyhl, B., Buchner, J., Radeloff, V.C., 2018. Mapping agricultural land abandonment from spatial and temporal segmentation of Landsat time series. Remote Sens. Environ. 210, 12–24. https://doi.org/10.1016/j.rse.2018.02.050.

Zazanashvili, N.R., Gagnidze, G., Nakhutsrishvili, 2000. Main types of vegetation zonation on the mountains of the Caucasus. Acta Phytogeogr. Suec. 85, 7–16.
Zhang, G., Biradar, C.M., Xiao, X., Dong, J., Zhou, Y., Qin, Y., Zhang, Y., Liu, F., Ding, M., Thomas, R.J., 2018. Exacerbated grassland degradation and desertification in Central Asia during 2000-2014. Ecol. Appl. 28, 442–456. https://doi.org/10.1002/eap.1660.
Zhang, R., Liang, T., Guo, J., Xie, H., Feng, Q., Aimaiti, Y., 2018b. Grassland dynamics in response to climate change and human activities in Xinjiang from 2000 to 2014. Sci. Rep. 8, 1–11. https://doi.org/10.1038/s41598-018-21089-3.
Zhang, Y., Wang, Q., Wang, Z., Li, J., Xu, Z., 2021. Dynamics and Drivers of Grasslands in the Eurasian Steppe during 2000 – 2014.
Zhou, W., Yang, H., Huang, L., Chen, C., Lin, X., Hu, Z., Li, J., 2017. Grassland degradation remote sensing monitoring and driving factors quantitative assessment in China from 1982 to 2010. Ecol. Indicat. 83, 303–313. https://doi.org/10.1016/j.ecolind.2017.08.019.
Zhu, Z., Woodcock, C.E., 2012. Object-based cloud and cloud shadow detection in Landsat imagery. Remote Sens. Environ. 118, 83–94. https://doi.org/10.1016/j.rse.2011.10.028.
Zhu, Z., Woodcock, C.E., 2014. Continuous change detection and classification of land cover using all available Landsat data. Remote Sens. Environ. 144, 152–171. https://doi.org/10.1016/j.rse.2014.01.011.
Zhu, Z., Piao, S., Myneni, R.B., Huang, M., Zeng, Z., Canadell, J.G., Ciais, P., Sitch, S., Friedlingstein, P., Arneth, A., Liu, R., Mao, J., Pan, Y., Peng, S., Peñuelas, J., Poulter, B., 2016. Greening of the Earth and its drivers. Nat. Clim. Change 6, 791–796. https://doi.org/10.1038/NCLIMATE3004.
Zhu, Z., Zhang, J., Yang, Z., Aljaddani, A.H., Cohen, W.B., Qiu, S., Zhou, C., 2019. Continuous monitoring of land disturbance based on Landsat time series. Remote Sens. Environ. 111116 https://doi.org/10.1016/j.rse.2019.03.009.